02,05

Properties of small magnetic hysteresis loop of granular HTSC: range of existence, remanent magnetization and relaxation of magnetization

© D.A. Balaev, S.V. Semenov, D.M. Gokhfeld, M.I. Petrov

Kirensky Institute of Physics, Federal Research Center KSC SB, Russian Academy of Sciences, Krasnoyarsk, Russia

E-mail: dabalaev@iph.krasn.ru

Received January 30, 2024
Revised January 30, 2024
Accepted January 31, 2024

The magnetic hysteresis loop of a granular high-temperature superconductor (HTSC) is determined both by the pinning of Abrikosov vortices in granules and by the penetration and trapping of a magnetic flux in the region of boundaries between granules. The subsystem of the intergranular boundaries of a granular HTSC is a Josephson medium, therefore, the trapped flux in it is Josephson vortices. Meissner currents shielding the external magnetic field cross the intergranular boundaries, which, together with the influence of pinned Josephson vortices, causes the so-called „small" magnetic hysteresis from the subsystem of intergranular boundaries. The properties of the small magnetic hysteresis of granular HTSC Y–Ba–Cu–O systems are studied in detail and described. Experimental conditions, including the magnetic background, have been determined in which the contribution of small hysteresis to the total magnetization of granular HTSC is significant or becomes vanishingly small. An explanation is given for the different manifestation of the contribution of small hysteresis at different magnetic prehistory. In conditions where the remanent magnetization is determined only by the trapping of the flux in the intergranular boundaries, the relaxation of magnetization associated with the dissipation of Josephson vortices is measured. The similarity and difference of such relaxation with the known relaxation associated with the dissipation of Abrikosov vortices are indicated. The shape of the small magnetic hysteresis loop was described using the critical state model.

Keywords: granular high-temperature superconductor, magnetic hysteresis, Josephson vortices, magnetization relaxation, pinning.

DOI: 10.61011/PSS.2024.04.58192.11

1. Introduction

The superconductor magnetic hysteresis loop, i.e., the dependence of magnetization on the external field $M(H)$, reflects its main characteristics important for practical applications. This applies both to applications in devices using a diamagnetic response, or a magnetic flux captured by a superconductor [1,2], and high-current applications (cables, short-circuit current limiters, electromagnetic motors) [3–10], since the height of the hysteresis loop $M(H)$ is proportional to the critical current density. Approaches to the description of the hysteresis behavior of the of superconductor magnetization have now been developed at a sufficient level to reliably determine the critical current density in magnetic fields and to define specific features related to the pinning mechanisms of Abrikosov vortices. Experimentally, the magnetization hysteresis of various superconducting materials has also been studied quite fully, this also applies to the class of high-temperature superconductors (HTSC).

Nevertheless, the granular HTSC systems have one specific feature of magnetic hysteresis observed in the region of weak fields, which has been studied to a much lesser extent than hysteresis in the range of moderate and strong magnetic fields. This paper will cover the so-called „small loop" of magnetic hysteresis [11–15]. A small hysteresis of the dependence $M(H)$ in classical granular HTSC systems based on yttrium and bismuth in the vicinity of the liquid nitrogen temperature is observed in the range of up to 10–20 Oe [11–15], up to several dozen Oersted at low temperatures [12,15]. It is quite logical that in weak fields, the diamagnetic response corresponds to the complete shielding of the field in a granular sample, while Meissner currents flow both in HTSC granules and across intergranular boundaries. Currents across the intergranular boundaries are caused by the Josephson effect, and the Josephson coupling between the granules is destroyed with an increase in the external field which results in the disappearance of a small hysteresis. The magnetic properties of granular HTSC in higher magnetic fields are determined by Meissner currents and magnetic flux capture only in HTSC granules.

The properties of small magnetic hysteresis of granular HTSC have not been studied fully enough despite the available qualitative description of magnetic properties of weak fields. The papers cited above [11–15] comprise a fairly representative list of studies of small magnetic hysteresis, and a number of features of magnetic properties in weak fields still require study and explanation. For

example, a recent paper [16] showed that the total magnetic hysteresis of the granular HTSC of the yttrium system is an unambiguous superposition of magnetizations from the intergranular boundaries (small hysteresis) and the magnetization of granules („large hysteresis“) only under certain conditions. In fact, the subsystems of granules and intergranular boundaries are connected, granules with „strong superconductivity“ generate „weak superconductivity“ (Josephson medium) in an intergranular medium. At the same time, the magnetic moments of the granules induce an additional field into the intergranular space, which results in the suppression of small hysteresis [16]. This work is devoted to a detailed study of the properties of small hysteresis of granular HTSC of the yttrium system, including the behavior of residual magnetization and its relaxation.

2. Experiment

Granular HTSC of the $Y_{0.98}Gd_{0.02}Ba_2Cu_3O_{7-\delta}$ composition was prepared from the corresponding oxides using standard solid-phase synthesis technology. The results of a detailed characterization of this sample are provided in Ref. [17]. According to the analysis of the powder diffraction pattern, the sample is single-phase, according to electron microscopy data, the average size of d_G superconducting granules is $4\,\mu$m. The temperature of transition T_C to the superconducting state was 93.8 K, the density of the transport critical current $j_C \sim 20\,\text{A/cm}^2$ at $T = 77.4\,\text{K}$. Hereinafter this sample is designated as YBCO-G. Another HTSC sample of the nominal formula $YBa_2Cu_3O_{7-\delta}$, studied in this paper, is described in detail in Ref. [16,18,19], for it $d_G \approx 10\,\mu$m, $T_C = 93.8\,\text{K}$, the density of the transport critical current $j_C(T = 77.4\,\text{K}) \sim 150\,\text{A/cm}^2$. Hereinafter this sample is designated as YBCO-S.

Magnetic measurements were performed using vibration magnetometer LakeShore VSM 8604. The samples for measurements were made in the shape of a ball with diameters of ≈ 2.5 mm (YBCO-G) and ≈ 3.5 mm (YBCO-S). The rate of field change for measuring dependencies $M(H)$ was $\sim 0.5-1$ Oe/s for the field area with a strength up to 150–200 Oe; the rate of change of the fields was ~ 5 Oe/s for measurements of fields with a maximum strength of up to 200–1000 Oe. Initially, the sample was cooled in a zero external field. For measuring a family of loops with different values of the maximum applied field $H_{\max}$, each subsequent value of the field $H_{\max}$ was greater than the previous one. The mode of measuring the residual magnetization at a constant temperature (Isothermal Remanence Magnetization — IRM) was used in some cases to measure the dependence of the residual magnetization (in the zero field) on the value of $H_{\max}$. The experimental values of the external field were adjusted taking into account the demagnetization factor of the sample.

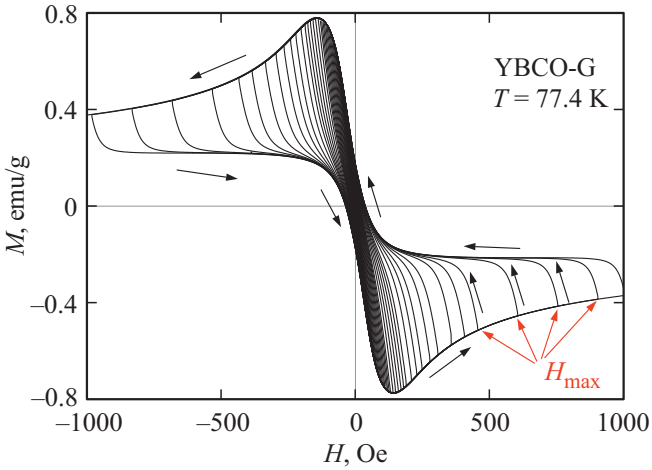

Figure 1. The magnetization hysteresis loops of the sample YBCO-G obtained with different values of the maximum applied field $\pm H_{\max}$ with a sequential increase of the value of $H_{\max}$. The black arrows show the direction of change of the external field, the red arrows show the values of the maximum field $H_{\max}$ in some magnetization reversal cycles.

3. Results and discussion

3.1. Large and small magnetic hysteresis loops and conditions of their coexistence

Figure 1 shows a family of magnetic hysteresis loops of the sample YBCO-G at $T = 77.4\,\text{K}$ obtained with different values of field $\pm H_{\max}$. The values of $H_{\max}$ increased sequentially by 5 Oe to $H_{\max} \approx 120$ Oe, at $H_{\max} > 120$ Oe field $H_{\max}$ increased by 10 Oe, at $H_{\max} > 180$ Oe, $H_{\max}$ increased by 20 Oe, and further in large fields by 50 and by 150 Oe (some points $+H_{\max}$ are shown in Figure 1).

The type of dependencies $M(H)$ shown in Figure 1 is typical for granular HTSC. The asymmetric shape of the dependences $M(H)$ relative to the abscissa axis is explained by the presence of a surface layer in granules in which the pinning of the Abrikosov vortices is weakened (the depth of this layer and the contribution from its equilibrium magnetization increase as the temperature approaches T_C) [20–24]. The data of Figure 1 are shown in Figure 2 on an enlarged scale in the vicinity of the point origin. The small magnetic hysteresis described in the Introduction is clearly visible in Figure 2, and, this hysteresis as a first approximation, is observed against the background of a linear diamagnetic response of superconducting granules.

Let's pay attention to one feature of the family of hysteresis loops with different values $H_{\max}$, highlighted in Figure 2. Arrows in Figure 2 indicate the characteristic arch-shaped features of the dependencies $M(H)$, corresponding to the extremes of the small magnetic hysteresis loop obtained by subtracting the diamagnetic response of superconducting granules (Figure 7). The data provided in Figure 2 show that the arc-like features become less pronounced with the growth of $H_{\max}$, and such features generally disappear

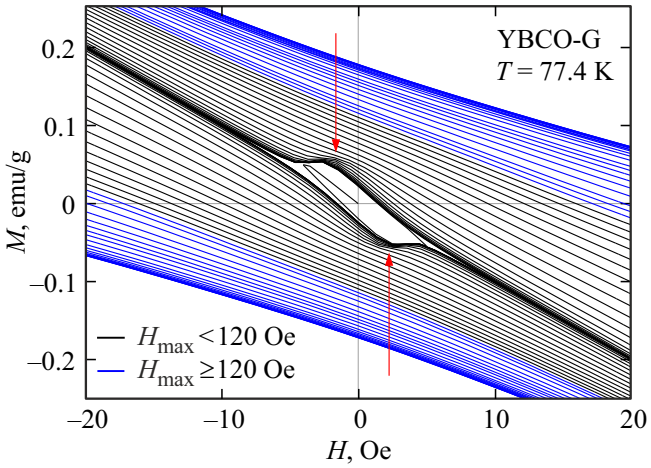

Figure 2. The data shown in Figure 1 is enlarged relative to the origin, the arrows indicate the arch-like feature discussed in the text. The dependencies $M(H)$ at $H_{\max} < 120$ Oe and at $H_{\max} \geq 120$ Oe are highlighted in color.

with sufficiently large values of $H_{\max}$. Mathematically, the absence of even a weakly expressed arch-shaped feature can be verified if the derivative of the function $dM(H)/dH$ has no extremum in the field region near $H = 0$. In our case, the derivative $dM(H)/dH$ of the sample YBCO-G does not show such extremes at $H^*_{\max} \sim 120$ Oe and large values $H_{\max}$. The dependencies $M(H)$ are highlighted in color in Figure 2 starting from $H^*_{\max} \sim 120$ Oe. The magnitude of the change of magnetization in the vicinity of the arch-shaped feature at values $H_{\max} \sim 10-40$ Oe is not small, and this change should also manifest itself against the background of dependence $M(H)$ in the vicinity of $H = 0$ at $H^*_{\max} \sim 120$ Oe. Therefore, there is a factor that reduces the contribution of small magnetic hysteresis to the overall dependence of $M(H)$.

The impact of the magnetic moments of superconducting granules on the intergranular boundaries is such factor as shown in Ref. [16]. The explanation is based on the concept of an effective field in an intergranular medium of granular HTSC [25–30]. Magnetic induction lines $\mathbf{B}_{\text{ind}}$ from the magnetic moments of granules $\mathbf{M}_G$ ($\mathbf{M}_G$ is the superposition of contributions from Abrikosov vortices and from Meissner currents in granules) close across intergranular intervals, see schematic representation in Figure 3, *a*. As a result, the field induced by moments $\mathbf{M}_G$ in the intergranular medium $\mathbf{B}_{\text{ind}}$ contributes to the total effective field $\mathbf{B}_{\text{eff}}$ in the intergranular medium: $\mathbf{B}_{\text{eff}} = \mathbf{H} + \mathbf{B}_{\text{ind}}$. The following expression is valid for the scalar value of the effective field taking into account the sign of the magnitude of magnetization M (Figure 3, *a*) [25–30]:

$$\mathbf{B}_{\text{eff}}(H) = H - \alpha \cdot 4\pi \cdot M(H). \qquad (1)$$

Here, the parameter α reflects the compression of the magnetic flux in the intergranular medium (Figure 3, *a*) of the granular HTSC, and the value of α reaches 12–20 due to this fact [25–30].

It follows from the analysis within the expression (1) that the magnetic moments of the granules have the main impact on the rather small range of existence of a small hysteresis through the field $\mathbf{B}_{\text{ind}}$ induced by them [16]. The impact of $\mathbf{M}_G$ results in the suppression of the response from small hysteresis and in the vicinity of $H = 0$ after

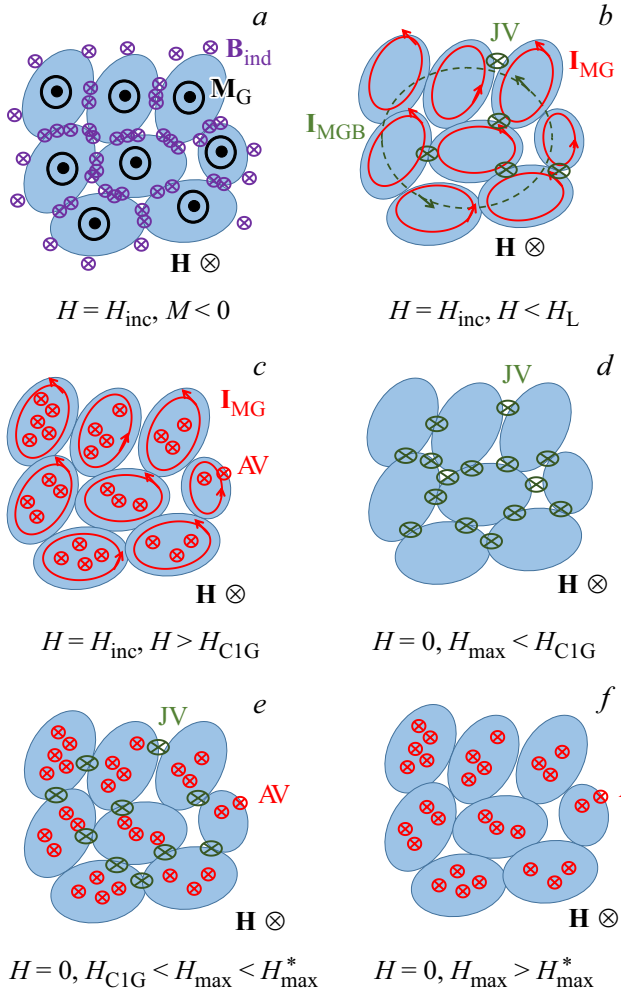

Figure 3. Schematic representation of a granular HTSC in an external field for various values of the external field and magnetic background. HTSC granules are shown by ovals, their places of contact correspond to intergranular boundaries. The cases of an increase of the external field $H = H_{\text{inc}}$ and the absence of an external field $H = 0$ are shown. (*a*) — the location of the directions of the magnetic moment vectors of granules $\mathbf{M}_G$ and magnetic induction lines $\mathbf{B}_{\text{ind}}$ (induced $\mathbf{M}_G$), closing through the intergranular boundaries; density $\mathbf{B}_{\text{ind}}$ corresponds to the general picture of the magnetic flux compression effect. (*b*) and (*c*) — the presence (absence) of Meissner currents across the intergranular boundaries $\mathbf{I}_{MGB}$ and inside the granules $\mathbf{I}_{MG}$, as well as the Josephson vortices JV and Abrikosov vortices AV in the specified ranges of the external field (range $H_L \approx 15-20$ Oe at (*b*) corresponds to $T = 77$ K). (*d*), (*e*), (*f*) — presence (absence) of the Josephson vortices JV and Abrikosov AV at $H = 0$ after application of the field $H_{\max}$ in the specified ranges.

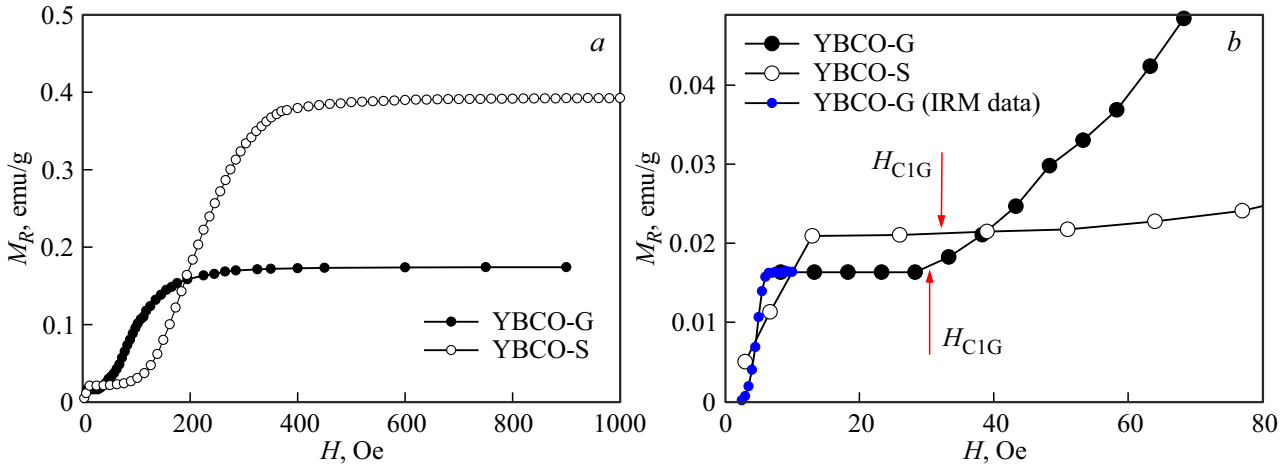

Figure 4. Dependences of the residual magnetization M_R on the magnitude of the maximum applied field $H_{\max}$ of the studied samples in the range of fields with the strength of up to 1 kOe (a) and in the range of small fields (b). The arrows on (b) indicate the points at which M_R deviates from a constant value, which corresponds to the beginning of the penetration of the field into HTSC granules.

the application of the field $H_{\max}$, i. e., disappearance of the arch-shaped dependence feature $M(H)$ at $H^*_{\max} \sim 120$ Oe and large values of $H_{\max}$. The value, $H^*_{\max}$, at which the arch-shaped feature on the dependency $M(H)$ disappears, is ~ 160 Oe for the sample of YBCO-S [16].

3.2. The behavior of the residual magnetization M_R depending on $H_{\max}$ and magnetic state in different ranges of the external field

Figure 4, *a, b* shows the dependencies $M_R(H_{\max})$. The dependence $M_R(H_{\max})$ reaches saturation in sufficiently large fields ($H_{\max} > 400$ Oe) (Figure 4, *a*). This is a typical behavior of the residual magnetization of superconductors of the second kind, in which, the general course of dependence $M(H)$ in a large range of fields does not depend on $H_{\max}$ at sufficiently large values of $H_{\max}$ [16,30–32]. A similar trend can be observed from the data provided in Figure 1: part of the hysteresis loop $M(H)$ in fields with the strength of less than $\sim \pm 200$ Oe at $H_{\max} > 400$ Oe almost does not depend on $H_{\max}$.

There is also an intermediate plateau in the area of small fields on the dependence $M_R(H_{\max})$ which is clearly visible on an enlarged scale in Figure 4, *b*. The dependence $M_R(H_{\max})$ has the form of *S*-shaped function (a double *S*-shaped function on large field scale). This part of the dependence $M_R(H_{\max})$ reflects the evolution of the residual magnetization of small hysteresis, i. e. magnetization of the subsystem of intergranular boundaries, and „intermediate“ plateau in the range $H_{\max} \sim 10-30$ Oe corresponds to a similar plateau $M_R(H_{\max})$ for the subsystem of granules in large fields ($H_{\max} > 400$ Oe).

The field at which the dependence $M_R(H_{\max})$ starts to deviate from a constant value in the intermediate plateau region (in fact, the loop of „large“ hysteresis begins to open) is the field of the first penetration into superconducting granules H_{C1G}. It can be determined from Figure 4, *b* that the value of H_{C1G} is ≈ 30 Oe for the sample of YBCO-G. The dependencies $M(H)$ with different values $H_{\max}$ for temperature 77.4 K for the sample YBCO-S are given in [16]. The corresponding dependencies $M_R(H_{\max})$ are shown in Figure 4. Figure 4, *b* shows that the value of H_{C1G} is ≈ 35 Oe [16].

It can be concluded based on a detailed examination of the data in Figure 2 (zooming in on the ordinate axis) that the range of existence of a small hysteresis is within $H_L \approx \pm 15-20$ Oe for YBCO-G sample. This range is $\approx \pm 20$ Oe for YBCO-S sample [16]. The given values of the field H_L are less than the field of the first penetration into the granules H_{C1G}. Therefore, the processes of field penetration into subsystems of intergranular boundaries and granules are strictly delimited. For this reason it is possible to specify different magnetic states for different ranges of the external field.

The external field penetrates into the subsystem of intergranular boundaries in the form of Josephson vortices (JV in Figure 3) in weak fields (small hysteresis) at $H \leq H_L$ [33–35]. Meissner currents flow in both subsystems, only in the case of small hysteresis, these currents $\mathbf{I}_{MGB}$ flow across the intergranular boundaries, shielding the external field throughout the sample, and in the case of large hysteresis, Meissner currents $\mathbf{I}_{MG}$ shield the field inside the granules. This is shown in the schematic representation in Figure 3, *b, c*. The superposition of Meissner currents ($\mathbf{I}_{MGB}$ and $\mathbf{I}_{MG}$) and Josephson vortices determines the shape of the small magnetic hysteresis loop. If the maximum field $H_{\max}$ has not exceeded H_{C1G}, then there are only Josephson vortices in the system after removal of the external field ($H = 0$).

The external field penetrates the granules in the form of Abrikosov vortices when the external field increases more than H_{C1G} (AV in Figure 3). And the contribution of small

hysteresis to the total magnetic hysteresis remains in small fields if the maximum field does not exceed the value of $H^*_{\max}$ ($H_{\max} < H^*_{\max}$, cl. 3.1), and two types of Meissner currents and vortices of two types (JV and AV) are present in a granular superconductor ($\mathbf{I}_{MGB}$ and $\mathbf{I}_{MG}$). The captured flow represents both Abrikosov vortices in granules and Josephson vortices for the condition $H_{\max} < H^*_{\max}$, after removal of the external field (at $H = 0$). In conditions when the small loop of magnetic hysteresis is strongly suppressed, i. e., at $H > H_L$ (Figure 3, *c*), and also near the zero field, after application of the field $H > H^*_{\max}$ (Figure 3, *f*), instead of the presence of pronounced pinned Josephson vortices (see cl. 3.1), it is probably necessary to talk about the complete penetration of the field into the intergranular area and the flow of Josephson vortices in the intergranular medium.

And finally, if $H_{\max} > H^*_{\max}$, then the captured flow is present only in granules in the form of Abrikosov vortices both with the increase of the field s (in the range of $H_{\max} > H^*_{\max}$) and with the decrease of the field, including the case of $H = 0$, (Figure 3, *f*).

3.3. Relaxation of the magnetization of the intergranular subsystem with the passage of time

The combination of the characteristic values of the external field presented above (cl. 3.2) (H_L, H_{C1G}, $H^*_{\max}$) allows determining the conditions of existence (i) only of the Josephson vortices and (ii) only of Abrikosov vortices (without Meissner currents) in the sample. Condition (i) is satisfied with $H = 0$ after application of the external field $H_{\max}$, not greater than H_{C1G}, see Figure 3, *d*. Condition (ii) is fulfilled with $H = 0$ after application of the external field exceeding the value $H^*_{\max}$ (120 and 160 Oe for YBCO-G and YBCO-S samples, respectively), see Figure 3, *f*. There are both Josephson vortices and Abrikosov vortices in the sample at $H = 0$ after application of field $H_{\max}$ of such magnitude that the double inequality $H_{C1G} < H_{\max} < H^*_{\max}$ holds, see Figure 3, *e*.

The magnetization of a superconductor demonstrates relaxation when this external parameter is constant like any other physical quantity with hysteresis behavior when an external parameter changes, in this case — at $H = \text{const}$. The relaxation of the magnetization of granular HTSC has been studied in sufficient detail, Ref. [25,26,30,36–39], however, as far as we know, the relaxation associated only with Josephson vortices has not been studied. This case corresponds to the condition (i) defined above. Based on this, we measured the evolution of the residual magnetization M_R over time in the zero field after the application of the field $H_{\max} = 15$ Oe (in this case $H_{\max} < H_{C1G}$). We also measured the relaxation associated with the dissipation of Abrikosov vortices to identify the features of magnetization relaxation associated with the dissipation of Josephson vortices. To do this, the residual magnetization M_R (in the zero field) was measured under condition (ii), while

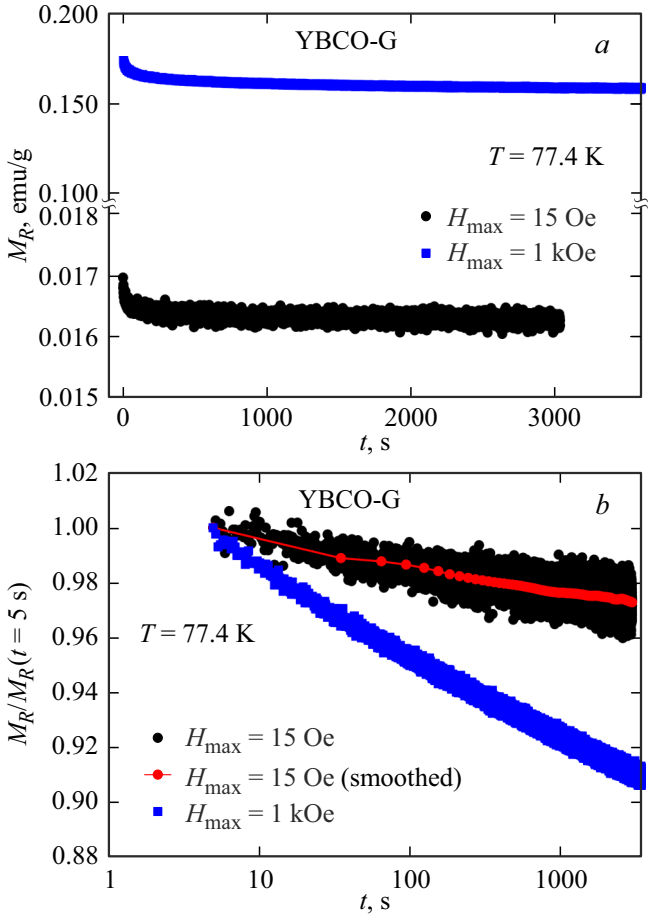

Figure 5. Dependence of the residual magnetization M_R on the time of the sample YBCO-G after application of the external field $H_{\max}$ of 15 Oe and 1 kOe. (*a*) — $M_R(t)$, (*b*) — data on M_R are normalized by the value at $t = 5$ s, abscissa axis — logarithmic scale. A smoothed dependence of $M_R(t)$ is also shown for data at $H_{\max} = 15$ Oe.

the external field was set to the value of $H_{\max} = 1$ kOe ($H_{\max} \gg H^*_{\max}$, $H_{\max} \gg H_{C1G}$).

The dependencies $M_R(t)$ under the specified conditions for YBCO-G and YBCO-S samples are shown in Figure 5, *a* and 6, *a*, respectively. The residual magnetization decreases quite significantly over time. The change of magnetization over time follows the logarithmic dependence $M(t)/M(t_0) \sim 1 - \text{const}\ln(t/t_0)$ quite well in the first approximation. This can be seen from the data in Figure 5, *b* and 6, *b*, where the dependencies $M_R(t)$ are given in coordinates $M_R(t)/M_R(t = 5\,\text{s})$, t, and a logarithmic scale is used along the abscissa axis. The data for the two studied samples are consistent, the magnetization associated with the dissipation of Abrikosov vortices (after $H_{\max} = 1$ kOe) decreases by $\approx 7-9\%$ over time ~ 3000 s, while this decrease for relaxation associated with Josephson vortices does not exceed 3%.

A logarithmic relaxation of magnetization is quite often observed with time starting from $t_0 \sim 10-100$ s in case of

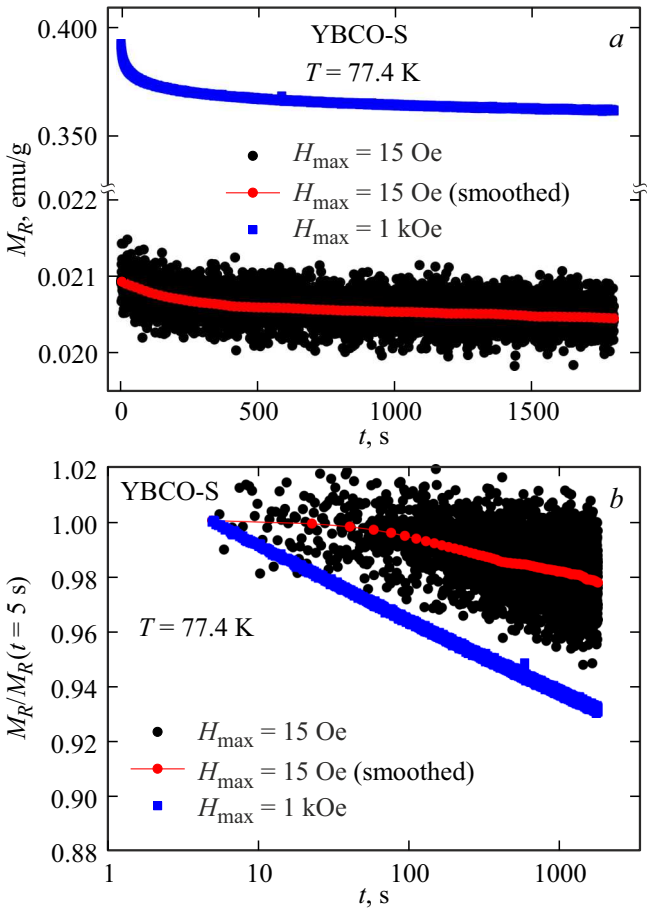

Figure 6. Dependence of the residual magnetization M_R on the time of the sample YBCO-S after application of the external field $H_{\max}$ of 15 Oe and 1 kOe. (a) — $M_R(t)$, (b) — data on M_R are normalized by the value at $t = 5$ s, abscissa axis — logarithmic scale. A smoothed dependence of $M_R(t)$ is also shown for data at $H_{\max} = 15$ Oe.

superconductors [37], although there are deviations from this dependence associated with the manifestation of a vortex glass type state [36,37] or quantum tunneling of vortices (at low temperatures) [38]. In the general case, the relaxation of magnetization is explained by the overcoming of the pinning potential (barrier) by vortices, i. e. by the thermal activation process. And it is possible to show [37] that the rate of change of magnetization (at $H = \text{const}$) depends on the energy value of the barrier U_P, which is crossed by the vortex:

$$M(t)/M(t_0) \sim 1 - (k_B \cdot T/U_P) \cdot \ln(t/t_0). \qquad (2)$$

Processing of data of Figure 5, b and 6, b using the expression (2) gives the following barrier values U_P: $U_{PJV} \approx 1.47$ eV for Josephson vortices (sample YBCO-G), 1.3 eV (sample YBCO-S) and $U_{PAV} \approx 0.52$ eV for Abrikosov vortices (sample YBCO-G) and 0.62 eV (sample YBCO-S). The values U_{PAV} are typical for granular HTSC of the yttrium system [37,25,30]. The higher value of U_{PJV} for the vortices of YBCO-S sample (compared to YBCO-G sample) is logically associated with a higher density of the transport critical current j_C of this sample. However, the main interesting and new result is that the energy barrier for the Josephson vortex is significantly (2–3 times) greater than the energy barrier for the Abrikosov vortex. Further detailed studies of the relaxation of magnetization corresponding to the processes in the subsystem of Josephson vortices with various external fields are needed.

3.4. Small magnetic hysteresis loop and critical current density

It is possible to conclude based on the results of cl. 3.1 and 3.2, that in the region of fields smaller than H_{C1G}, the dependence of $M(H)$ of granular HTSC is additive to contributions from subsystems of intergranular boundaries $M_{GB}(H)$ (small hysteresis) and from granules $M_G(H)$: $M(H) = M_{GB}(H) + M_G(H)$. In this case, $M_G(H) = \chi \cdot H$, where $\chi < 0$. Therefore, the function $M_{GB}(H)$ can be correctly defined by expression

$$M_{GB}(H) = M(H) - \chi \cdot H. \qquad (3)$$

Figure 7, a shows the dependencies $M(H)$ and $M_G(H) = \chi \cdot H$, and also a small magnetic hysteresis loop $M_{GB}(H)$ of YBCO-G obtained using the expression (3). The dependences $M(H)$ in Figure 7, b in the region of the existence of small hysteresis for YBCO-S sample at temperatures 77.4, 85 and 87 K. Figure 8 illustrates the loops of small magnetic hysteresis (dependences$M_{GB}(H)$) of YBCO-G sample (Figure 8, a) and YBCO-S sample (Figure 8, b) at $T = 77.4$, 85 and 87 K.

The shape of the loop of small magnetic hysteresis (Figure 7) has its characteristic differences from the corresponding hysteresis of HTSC granules (Figure 1). This is not surprising, since the small and large loops are attributable to the responses from completely different superconducting subsystems. At the same time, the characteristic pattern of magnetic flux penetration of both subsystems into a superconductor is similar in a granular sample. The critical state model [40] works both for Abrikosov vortices penetrating granules in sufficiently large fields [41] and for Josephson vortices penetrating a granular superconductor in small fields [42,43]. Therefore, it is possible to expect that the model describing the magnetization of granules will also describe the magnetization of the subsystem of intergranular boundaries.

The density of the intragranular critical current j_{CG} can be estimated based on the height of the large hysteresis loop ΔM in Figure 1, since the relationship between j_C and ΔM is established in the critical state model [40]. The formula $j_{CG} = 30\Delta M \rho_G / d_G$ is used for polycrystalline samples, where ρ_G — the physical density of the granule material in g/cm^3, and ΔM — magnetization in emu/g [44]. $j_{CG} = 1.4 \cdot 10^5$ A/cm^2 is obtained for YBCO-G and $j_{CG} = 2 \cdot 10^5$ A/cm^2 is obtained for YBCO-S.

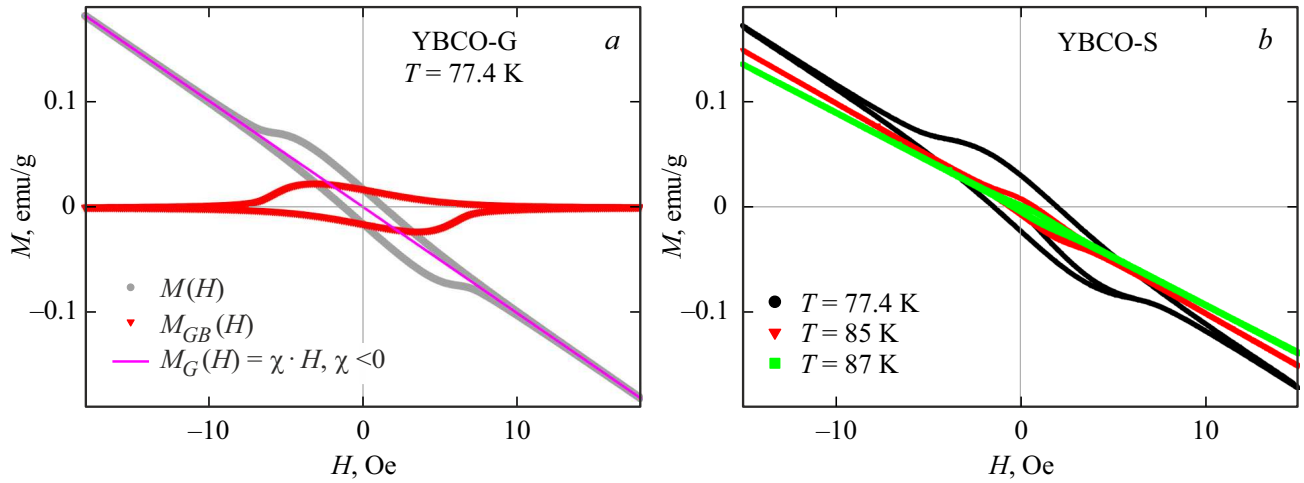

Figure 7. *a* — magnetic hysteresis loop $M(H)$ of YBCO-G sample with $H_{max} = \pm 20$ Oe, linear dependence $M_G(H) = \chi H$, corresponding to the diamagnetism of HTSC granules ($\chi < 0$), and the contribution from the subsystem of intergranular boundaries $M_{GB}(H)$, obtained after deducting the diamagnetic contribution from granules; *b* — magnetic hysteresis loops $M(H)$ of YBCO-S sample with $H_{max} = \pm 15$ Oe and the temperatures indicated on the legend.

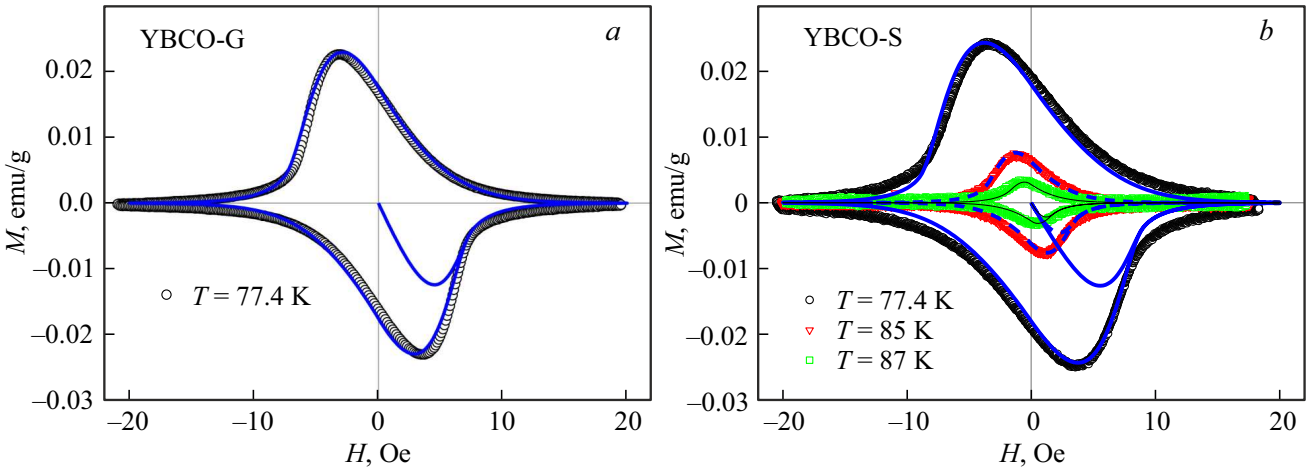

Figure 8. Small magnetic hysteresis loops — the dependences $M_{GB}(H)$ obtained after deducting the diamagnetic contribution from granules for YBCO-G sample at $T = 77.4$ K (*a*) and YBCO-S sample at temperatures of 77.4, 85, 87 K (*b*). The lines are calculated using the critical state model with exponential dependence j_{CGB} on H.

Similarly, the density of the intergranular critical current j_{CGB} can be estimated based on the height of the hysteresis loops ΔM in Figure 8. For the case of a ball $j_C = 35\Delta M\rho/d_{\text{circle}}$ [45], where d_{circle} is the diameter of the ball, ρ is the density of the sample. This formula gives the values $j_{CGB} = 23$ A/cm^2 for YBCO-G and $j_{CGB} = 49$ A/cm^2 for YBCO-S. The formula is obtained with the assumption of the independence of the critical current from the magnetic field (bin approximation), therefore the estimated values are underestimated [44.45]. Therefore, the density of the critical current in the subsystem of intergranular boundaries is more than three orders of magnitude less than the density of the intragranular critical current.

A more accurate estimate of j_{CGB} can be obtained by assuming a field dependence of the critical current density. We described the magnetization loops in Figure 8 using the critical state model in variant [24]. The exponential dependence of the critical current density on the magnetic field $j_{CGB} = j_{C0}\exp(-B/B_0)$ was used for the calculations. The applied model considers an infinitely long cylinder, rather than the ellipsoid geometry appropriate for these samples. However, the magnetization of a spherical sample can be qualitatively reproduced by considering an equivalent cylinder [16] with a diameter of $d_{\text{eff}} = \pi d_{\text{circle}}/4$. The impact of the demagnetization factor and the effective field was taken into account using an adjustment coefficient k_H, which establishes the difference between the field H in the model and the magnitude of the external field for the

Parameters used in the description of magnetization loops in Figure 8

Parameters	j_{C0}, A/cm^2	B_0, Oe	k_H	d_{eff}, cm
YBCO-G (77 K)	90	0.63	4	0.194
YBCO-S (77 K)	240	0.65	4	0.131
YBCO-S (85 K)	40	0.4	4	0.131
YBCO-S (87 K)	12	0.35	4	0.131

samples. It is possible to state that the parameter k_H determines the relationship of the effective fields for the cylinder and the ball.

The calculated hysteresis magnetization loops are plotted on charts together with experimental dependences in Figure 8. The adjustment parameters used are listed in the table. The value j_{C0} was the main adjustment parameter determining the magnetization values for the lower and upper branches of the loop. The parameter B_0 determines the loop collapse rate. The height of the loop ΔM becomes less than 1% of ΔM in the zero field at $H = H_L$, this is achieved with the value $B_0 \approx H_L/(7k_H)$.

4. Conclusion

A detailed study of the minor hysteresis loops of the magnetization of granular HTSC systems revealed the following patterns of behavior of a small magnetic hysteresis loop.

The small magnetic hysteresis caused by the capture of Josephson vortices by intergranular boundaries (Josephson medium) makes a significant contribution to the overall magnetization in the region of small fields. It exists when the field is cycled in the range up to a certain value H_L, $H_L \sim 15-20$ Oe at the liquid nitrogen temperature. Under these conditions, only the subsystem of intergranular boundaries determines the hysteresis behavior of the magnetization of a granular HTSC. The hysteresis associated with the granule subsystem begins to unfold in fields approximately twice as large as H_L. At the same time, the impact of small hysteresis from the subsystem of intergranular boundaries remains noticeable in weak fields (in the vicinity of $H \sim 0$), but becomes vanishingly small if the maximum applied field reaches a certain value $H^*_{\max}$. The value of $H^*_{\max}$ can be $\sim 120-170$ Oe at the liquid nitrogen temperature. In other words, a small magnetic hysteresis collapses in the range of fields large H_L, and also in the entire range of fields under the impact of magnetic prehistory, in which the maximum applied field reached the value $H^*_{\max}$. The impact of the magnetic moments of the granules on the total effective field within the intergranular boundaries is the main factor influencing the described collapse of small hysteresis. The effective field in the intergranular boundaries is mainly determined by the magnetization of the granules due to the impact of compression of the magnetic flux and significantly exceeds the external field.

It is possible to determine the conditions of existence in a granular sample (i) only of Josephson vortices, (ii) only of Abrikosov vortices, or, in other cases, their co-existence with Meissner currents since the characteristic values of the fields in which the hysteresis response of magnetization appears in the subsystems of intergranular boundaries and granules are different. This allowed us for recording the relaxation of the residual magnetization over time associated with the dissipation of Josephson vortices. The value determining the rate of relaxation of magnetization was found to be in 2–3 three times greater for Josephson vortices than the same value for Abrikosov vortices.

It is possible to correctly identify the hysteresis loop associated with the subsystem of intergranular boundaries using the experimental data. It is possible to describe the shape of a small magnetic hysteresis loop using the same critical state model that is used to calculate the magnetization of bulk superconductors and polycrystalline HTSC. The values of the critical current density obtained from the critical state model are consistent with the values of the transport critical current.

The studied samples can be considered representative of granular HTSC materials of the yttrium system. For this reason the results obtained should be considered as typical for ceramic HTSC samples obtained using standard methods with a structure of 1–2–3.

Funding

The study was performed under the state assignment of the Institute of Physics, Siberian Branch of RAS. Magnetic measurements were performed using the equipment of the Krasnoyarsk Regional Center for Collective Use, Krasnoyarsk Scientific Center, Siberian Branch of the Russian Academy of Sciences.

Conflict of interest

The authors declare that they have no conflict of interest.

References

[1] P. Bernstein, J. Noudem. Supercond. Sci. Technol. **33**, 033001 (2020).
[2] D.M. Gokhfeld, M.R. Koblishka, A. Koblishka-Veneva. FMM **121**, 1026 (2020). (in Russian).
[3] G. Wang, M.J. Raine, D.P. Hampshire. Supercond. Sci. Technol. **31**, 024001 (2018).
[4] J. Huang, H. Wang. Supercond. Sci. Technol. **30**, 114004 (2017).
[5] E.Y. Klimenko. Phys.-Usp. **191**, 861 (2021). (in Russian).
[6] E.Y. Klimenko. Sverkhprovodimost': fundamental'nye i prikladnye issledovaniya *1*, 6 (2023). (in Russian).
[7] E.P. Kurbatova. Sverkhprovodimost': fundamental'nye i prikladnye issledovaniya *1*, 40 (2023). (in Russian).

[8] G.G. Sotelo, G. dos Santos, F. Sass, B.W. França, D.H. Nogueira Dias, M.Z. Fortes, A. Polasek, R. de Andrade Jr. Superconductivity **3**, 100018 (2022).
[9] I.V. Martirosyan, I.K. Mikhailova, S.V. Pokrovsky, I.A. Rudnev. Sverkhprovodimost': fundamental'nye i prikladnye issledovaniya **1**, 31 (2023). (in Russian).
[10] N.S. Ivanov, S.V. Zhuravlev, V.A. Kaderov, N.A. Malevich, B. Duine. Sverkhprovodimost': fundamental'nye i prikladnye issledovaniya *1*, 56 (2023). (in Russian).
[11] G.E. Gough, M.S. Colclough, D.A. O'Connor, E. Wellhoffer, N.McN. Alford, T.W. Button. Cryogenics **31**, 119 (1991).
[12] J. Jung, M.-K. Mohamed, S.C. Cheng, J.P. Franck. Phys. Rev. B **42**, 6181 (1990).
[13] I. Edmondt, L.D. Firh. J. Phys: Condens. Matter. **4**, 3813 (1992).
[14] F. Pèrez, X. Obradors, J. Fontcuberta, X. Bozec, A. Fert. Supercond. Sci. Technol. **9**, 161 (1996).
[15] B. Andrzejewski, E. Guilmeau, C. Simon. Supercond. Sci. Technol. **14**, 904 (2001).
[16] D.A. Balaev, S.V. Semenov, D.M. Gokhfeld, M.I. Petrov. ZhETF **165**, *2*, 258 (2024). (in Russian).
[17] D.M. Gokhfeld, S.V. Semenov, I.V. Nemtsev, I.S. Yakimov, D.A. Balaev. J. Supercond. Nov. Magn. **35**, 2679 (2022).
[18] S.V. Semenov, A.D. Balaev, D.A. Balaev. J. Appl. Phys. **125**, 033903 (2019).
[19] S.V. Semenov, D.A. Balaev. FTT **62**, *7*, 1008 (2020). (in Russian).
[20] E.V. Blinov, Yu.P. Stepanov, K.B. Traito, L.S. Vlasenko, R. Laiho, E. Lahderanta. JETP **106**, 790 (1994).
[21] F.F. Ternovsky, L.N. Shekhata. ZhETF **62**, 2297 (1972). (in Russian).
[22] L. Burlachkov, A.E. Koshelev, V.M. Vinokur. Phys. Rev. B **54**, 6750 (1996).
[23] A.A. Elistratov, I.L. Maksimov. FTT **42**, 196 (2000). (in Russian).
[24] D.M. Gokhfeld. FTT **56**, 2298 (2014). (in Russian).
[25] D.A. Balaev, S.I. Popkov, E.I. Sabitova, S.V. Semenov, K.A. Shaykhutdinov, A.V. Shabanov, M.I. Petrov. J. Appl. Phys. **110**, 093918 (2011).
[26] D.A. Balaev, A.A. Dubrovsky, K.A. Shaikhutdinov, S.I. Popkov, D.M. Gokhfeld, Y.S. Gokhfeld, M.I. Petrov. ZhTF **135**, 271 (2009). (in Russian).
[27] S.V. Semenov, D.A. Balaev. Physica C **550**, 19 (2018).
[28] S.V. Semenov, D.A. Balaev. J. Supercond. Nov. Magn. **32**, 2409 (2019).
[29] S.V. Semenov, D.A. Balaev, M.I. Petrov. FTT **63**, *7*, 854 (2021). (in Russian).
[30] D.A. Balaev, S.V. Semenov, D.M. Gokhfeld. J. Supercond. Nov. Magn. **36**, 1631 (2023).
[31] H. Dersch, G. Blatter. Phys. Rev. B **38**, *16*, 11391 (1988).
[32] D.A. Balaev, S.V. Semenov, D.M. Gokhfeld. FTT **64**, *12*, 1882 (2022). (in Russian).
[33] E.B. Sonin. Pisma ZhETF **47**, 415 (1988). (in Russian).
[34] A. Barone, G. Paterno. Josephson effect. Mir, M. (1984). 639 p. (in Russian).
[35] Yu.M. Tsipenyuk. Fizicheskie osnovy sverkhprovodimosti. MFTI, M. (2003). 160 p. (in Russian).
[36] G. Blatter, M.V. Feigel'man, V.B. Gekshkebein, A.I. Larkin, V.M. Vinokur. Rev. Mod. Phys. **66**, 1125 (1994).
[37] Y. Yeshurun, A.P. Malozemoff, A. Shaulov. Rev. Mod. Phys. **68**, 911 (1996).
[38] X.X. Zhang, A. Garcia, J. Tejada, Y. Xin, G.F. Sun, K.W. Wong. Phys. Rev. B **152**, 1325 (1995).
[39] L. Burlachkov, S. Burov. Phys. Rev. B **103**, 024511 (2021).
[40] C.P. Bean. Rev. Mod. Phys. **36**, 31 (1964).
[41] V.V. Valkov, B.P. Khrustalev. ZhETF **107**, 1221 (1995). (in Russian).
[42] K.-H. Müller. Physica C **159**, 717 (1989).
[43] K.-H. Müller, D.N. Matthews, R. Driver. Physica C **191**, 339 (1992).
[44] D.M. Gokhfeld. J. Supercond. Nov. Magn. **36**, 1089 (2023).
[45] K.V. Bhagwat, P. Chaddah. Physica C **224**, 155 (1994).

Translated by A.Akhtyamov